Collisions inside subfemtosecond laser pulses

L. Kocbach[1], L.B. Madsen[2] and J.P. Hansen[1]

[1] **University of Bergen, Norway**

[2] **University of Århus, Denmark**

The Nobel Prize in Chemistry 1999

The Royal Swedish Academy of Sciences has awarded the 1999 Nobel Prize in Chemistry to Professor Ahmed H. Zewail for his studies of transition states of chemical reactions by femtosecond spectroscopy.

The Nobel Prize in Chemistry 1999

The Royal Swedish Academy of Sciences has awarded the 1999 Nobel Prize in Chemistry to Professor Ahmed H. Zewail for his studies of transition states of chemical reactions by femtosecond spectroscopy.

Zewail's technique uses what can be thought of as the world's fastest camera. The "shutter speed" of such a camera must be extremely high since molecules are very small (about 10^{-9} m) and move extremely rapidly (1000 m/s). To obtain a sharp "image" of the molecules in the course of a chemical reaction requires a femtosecond (10^{-15} s) shutter speed.

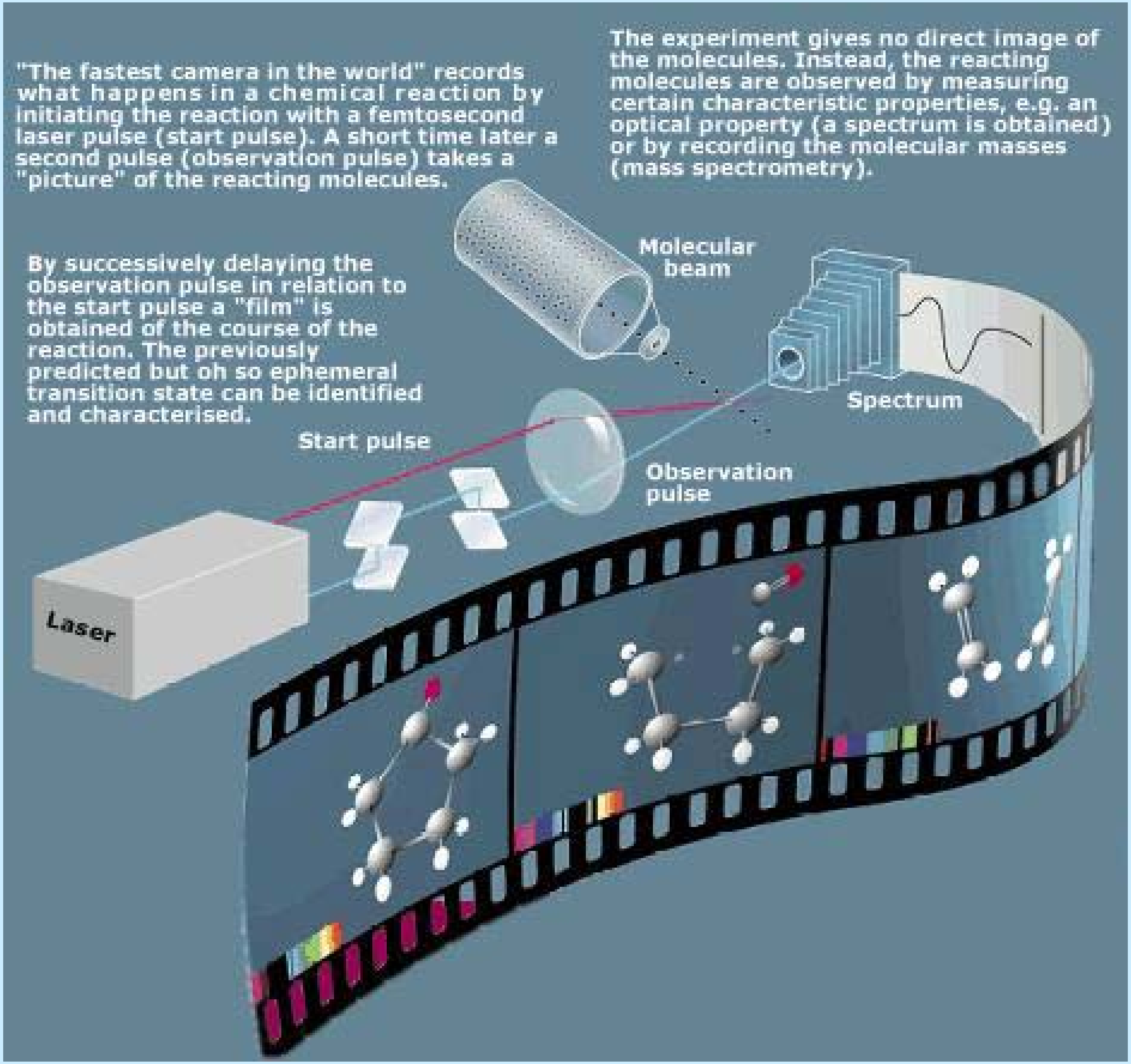
"The fastest camera in the world" records what happens in a chemical reaction by initiating the reaction with a femtosecond laser pulse (start pulse). A short time later a second pulse (observation pulse) takes a "picture" of the reacting molecules.
The experiment gives no direct image of the molecules. Instead, the reacting molecules are observed by measuring certain characteristic properties, e.g. an optical property (a spectrum is obtained) or by recording the molecular masses (mass spectrometry).
By successively delaying the observation pulse in relation to the start pulse a "film" is obtained of the course of the reaction. The previously predicted but oh so ephemeral transition state can be identified and characterised.
Molecular beam
Spectrum
Start pulse
Observation pulse
Laser

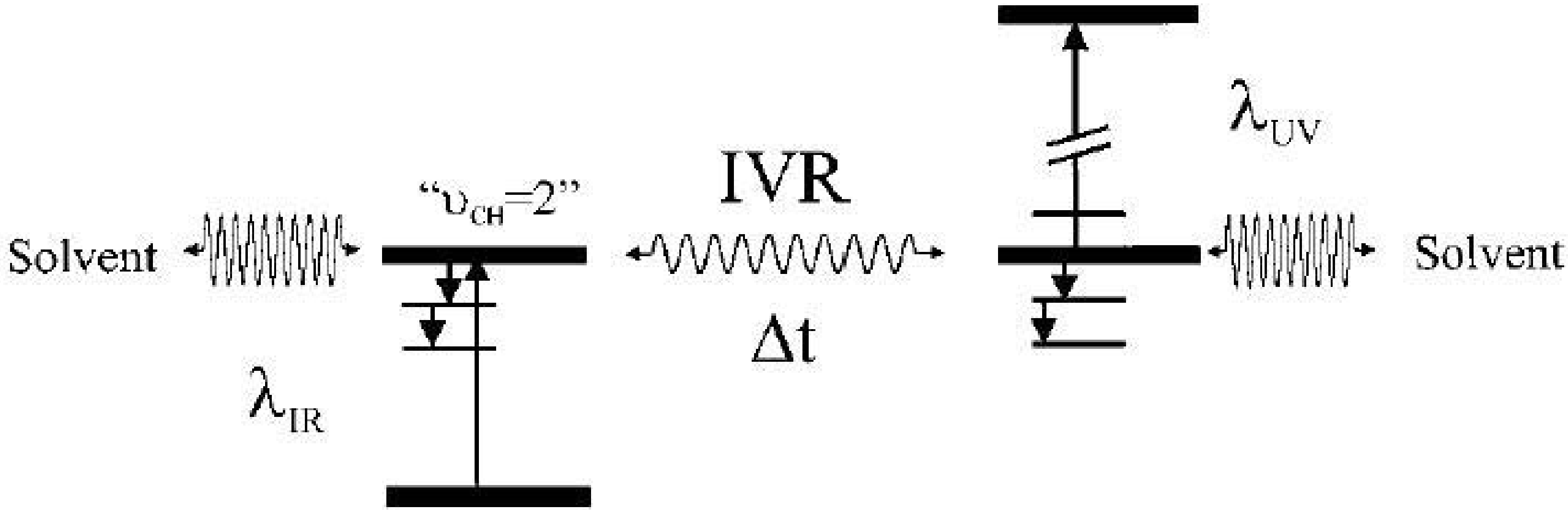

Figure 1. Experimental scheme. In our pump-and-probe experiment the first near-IR femtosecond-laser pulse prepares a vibrationally excited molecule with an energy of 4000−6000 cm^{-1} in its ground electronic state, and a second laser pulse, tuned to the red wing of the electronic transition in the UV, measures the change in absorption induced by the first laser pulse.

Few Cycles Light Pulses

FIG. 1. Focusing of few-cycle ultrashort light pulses delivered in a collimated laser beam by a parabolic mirror, producing a “light bullet” with transverse and longitudinal dimensions of the order of a few microns. This extreme spatial and temporal confinement of light creates optical-field strengths sufficient to lower the Coulomb barrier of atoms and to tunnel-ionize an outer electron at moderate pulse energy levels.

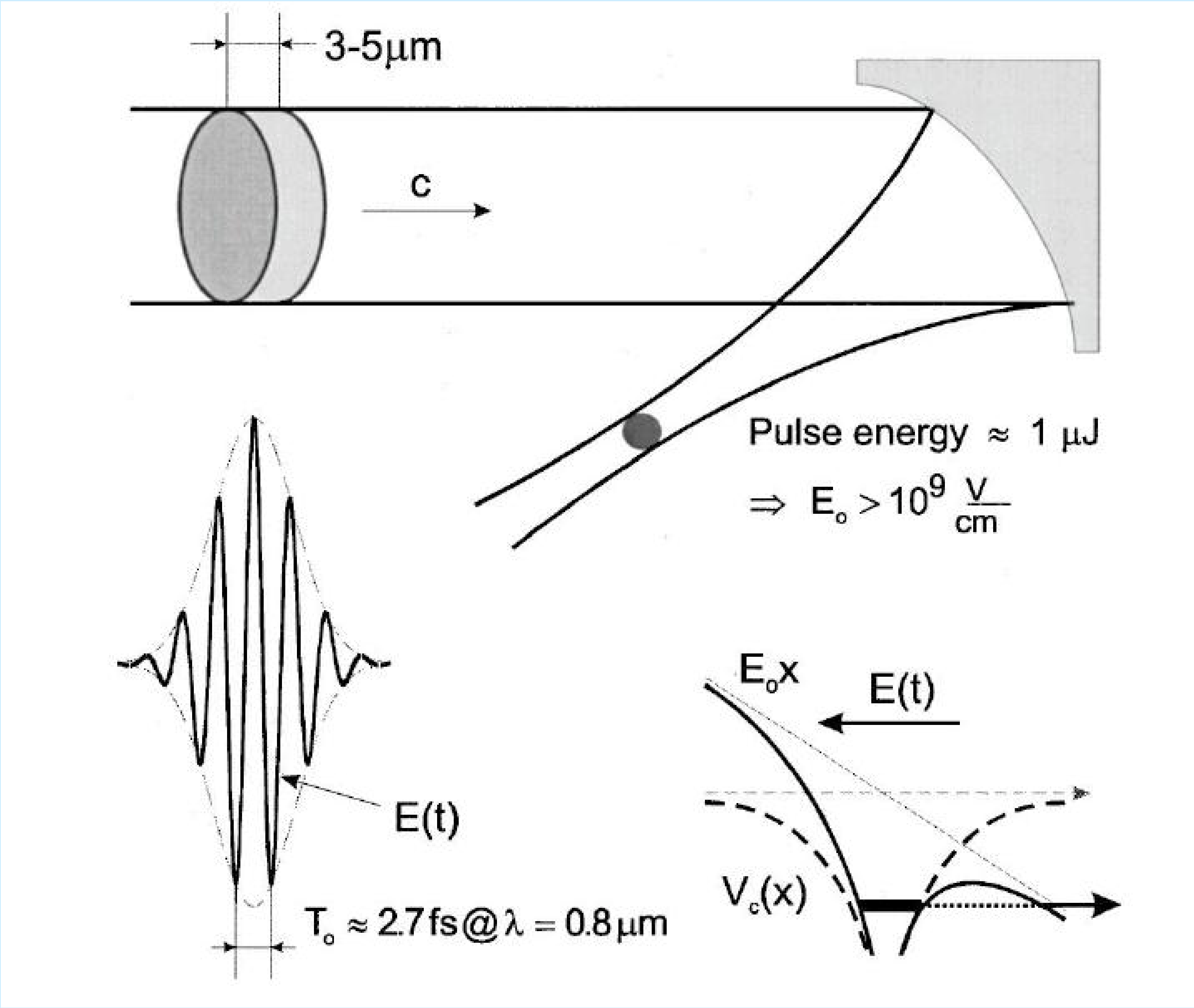
3-5μm
c
Pulse energy ≈ 1 μJ
⇒ $E_o > 10^9 \frac{V}{cm}$
E(t)
$T_o \approx 2.7\,fs @ \lambda = 0.8\,\mu m$
$E_o x$
E(t)
$V_c(x)$

VOLUME 89, NUMBER 9 PHYSICAL REVIEW LETTERS 26 AUGUST 2002

Excitation in Ion-Atom Collisions Inside Subfemtosecond Laser Pulses

L. B. Madsen,[1] J. P. Hansen,[2] and L. Kocbach[2]
[1]*Institute of Physics and Astronomy, University of Aarhus, 8000 Århus C, Denmark*
[2]*Institute of Physics, University of Bergen, Allégaten 55, 5007 Bergen, Norway*
(Received 24 January 2002; revised manuscript received 19 June 2002; published 9 August 2002)

We discuss new excitation mechanisms in energetic ion-atom collisions embedded in short laser pulses. For comparable duration and strength of the pulse and collisional interaction, the laser field will probe and modify the interaction between projectile and target. Coherence effects emerge, insight into reaction dynamics is gained, and new dynamical features are discovered. As an example, we show (i) how a propensity rule for *s*-*p* excitation can be dramatically changed, and (ii) how the presence of the laser pulse modifies the ionization process in ion-atom collisions.

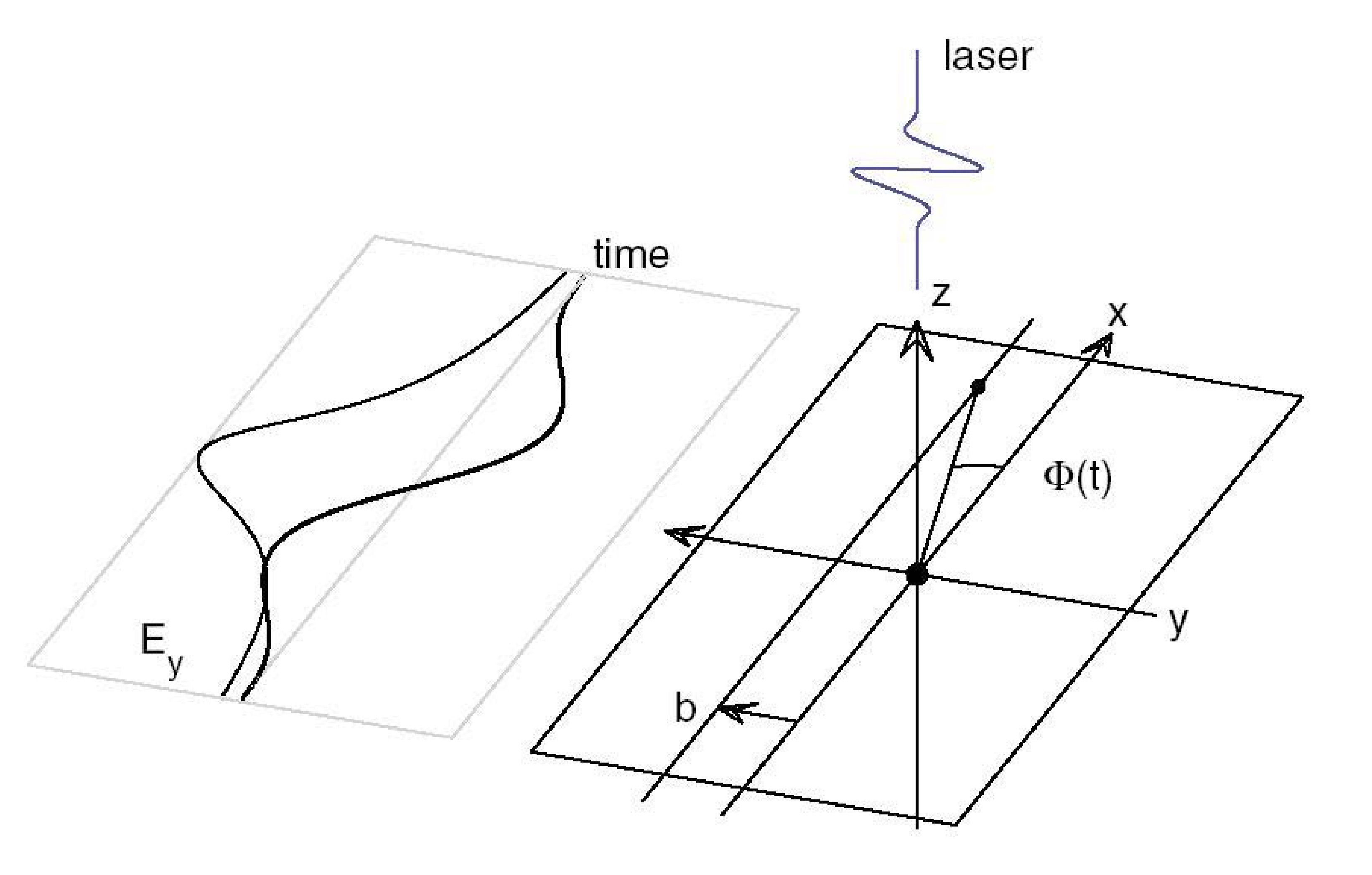

Collision and laser pulse combined

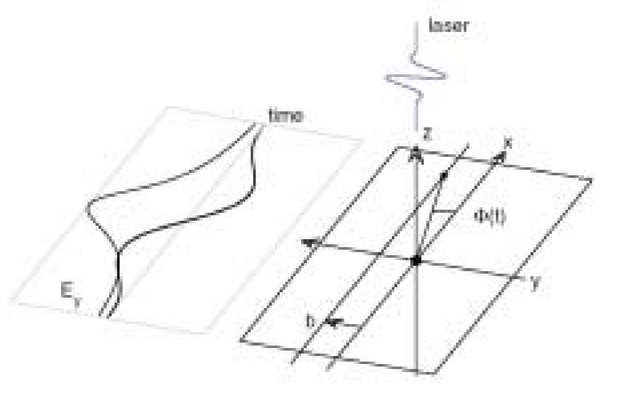
laser
time
z
x
Φ(t)
y
b
E_y

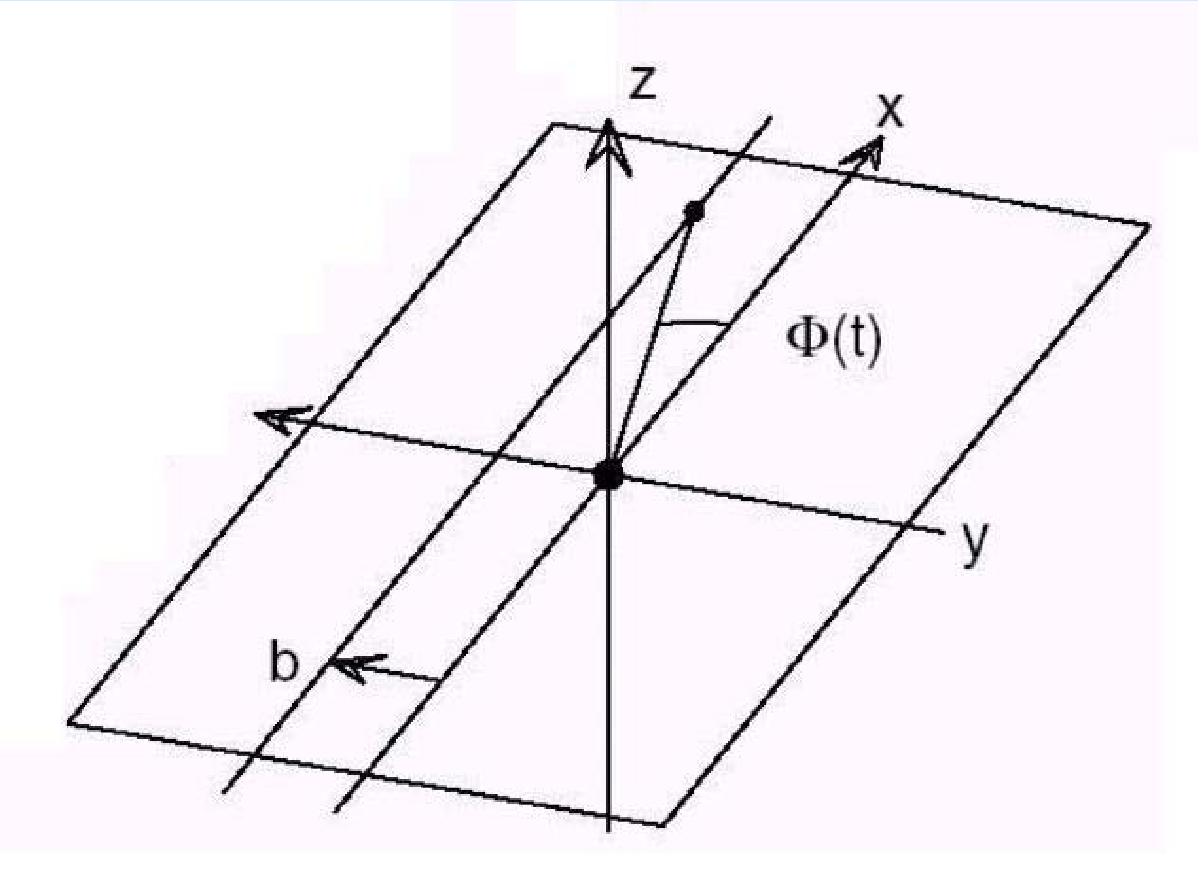
z
x
Φ(t)
y
b

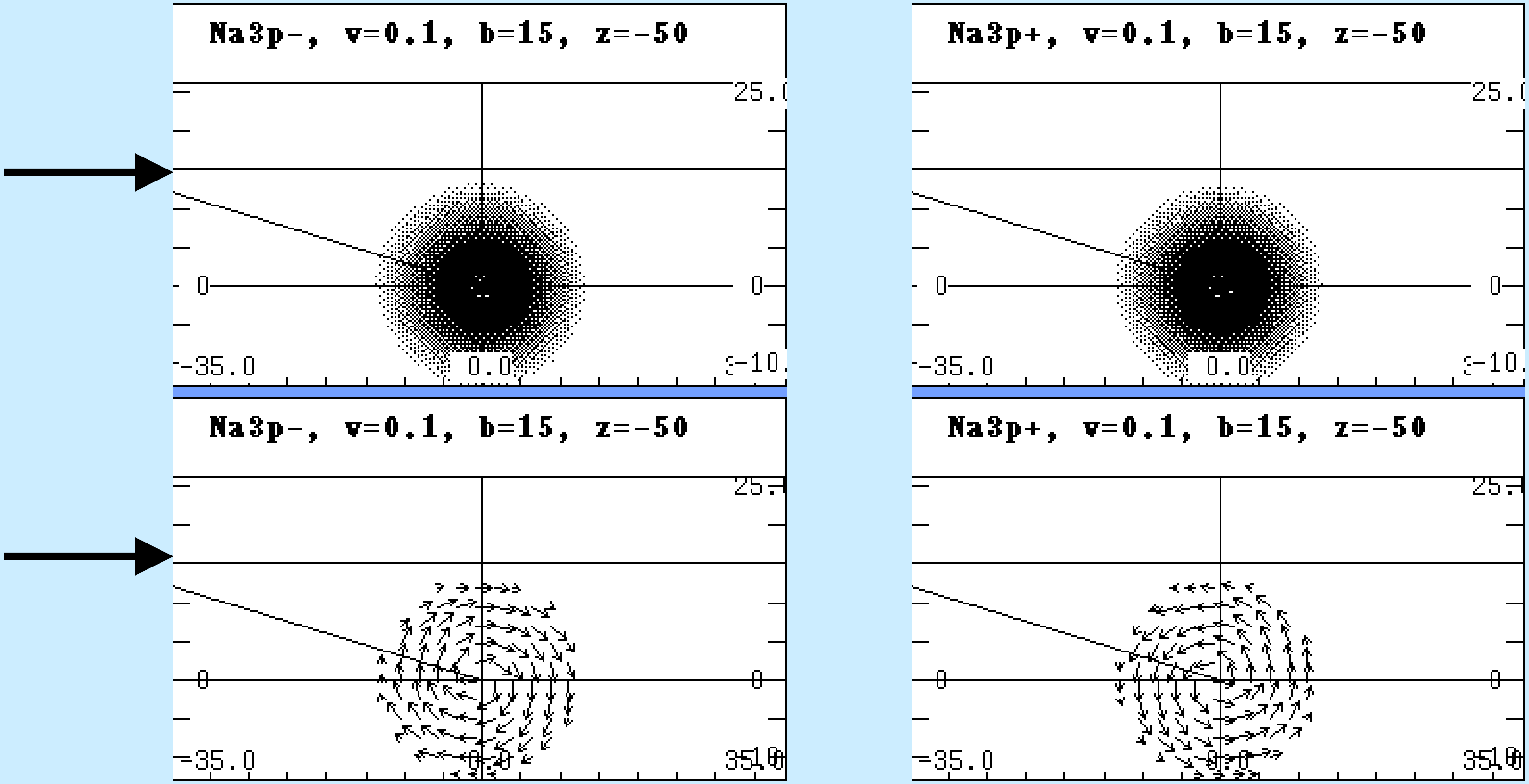
Na3p-, v=0.1, b=15, z=-50
Na3p+, v=0.1, b=15, z=-50
Na3p-, v=0.1, b=15, z=-50
Na3p+, v=0.1, b=15, z=-50
-35.0
0.0
0

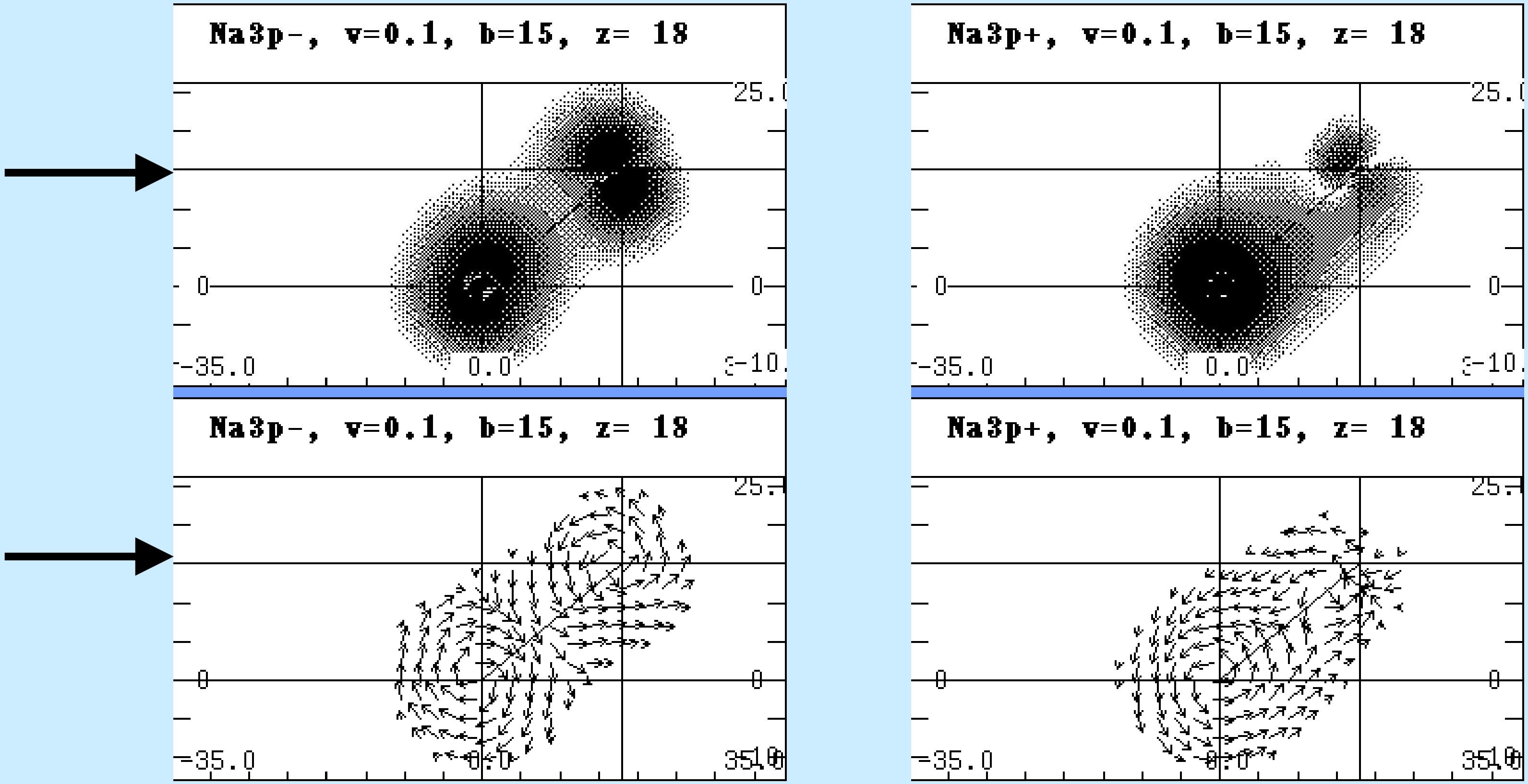
Na3p-, v=0.1, b=15, z= 18
Na3p+, v=0.1, b=15, z= 18
Na3p-, v=0.1, b=15, z= 18
Na3p+, v=0.1, b=15, z= 18
25.0
0
-35.0
0.0

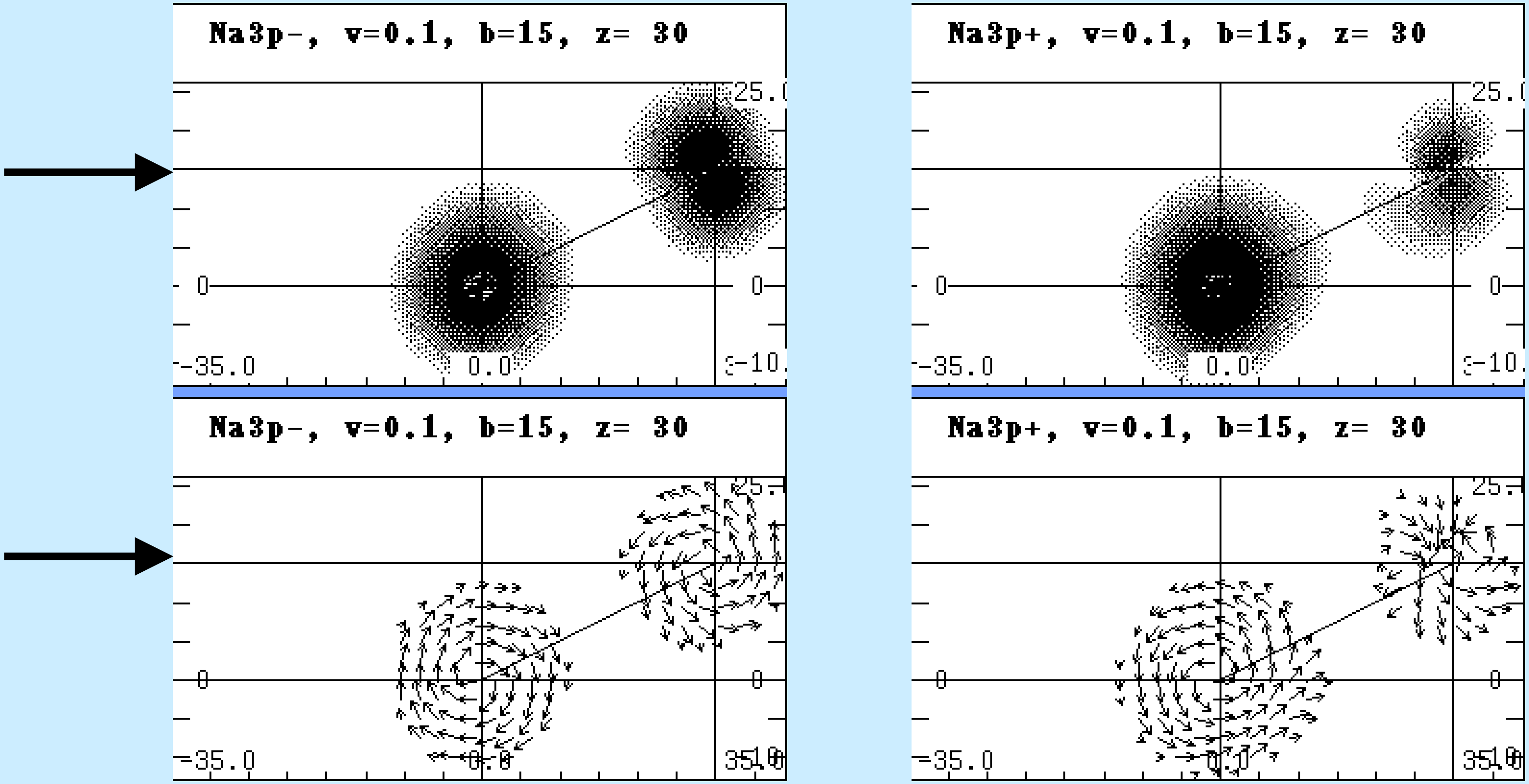
Na3p-, v=0.1, b=15, z= 30
Na3p+, v=0.1, b=15, z= 30
Na3p-, v=0.1, b=15, z= 30
Na3p+, v=0.1, b=15, z= 30
-35.0
0.0
0

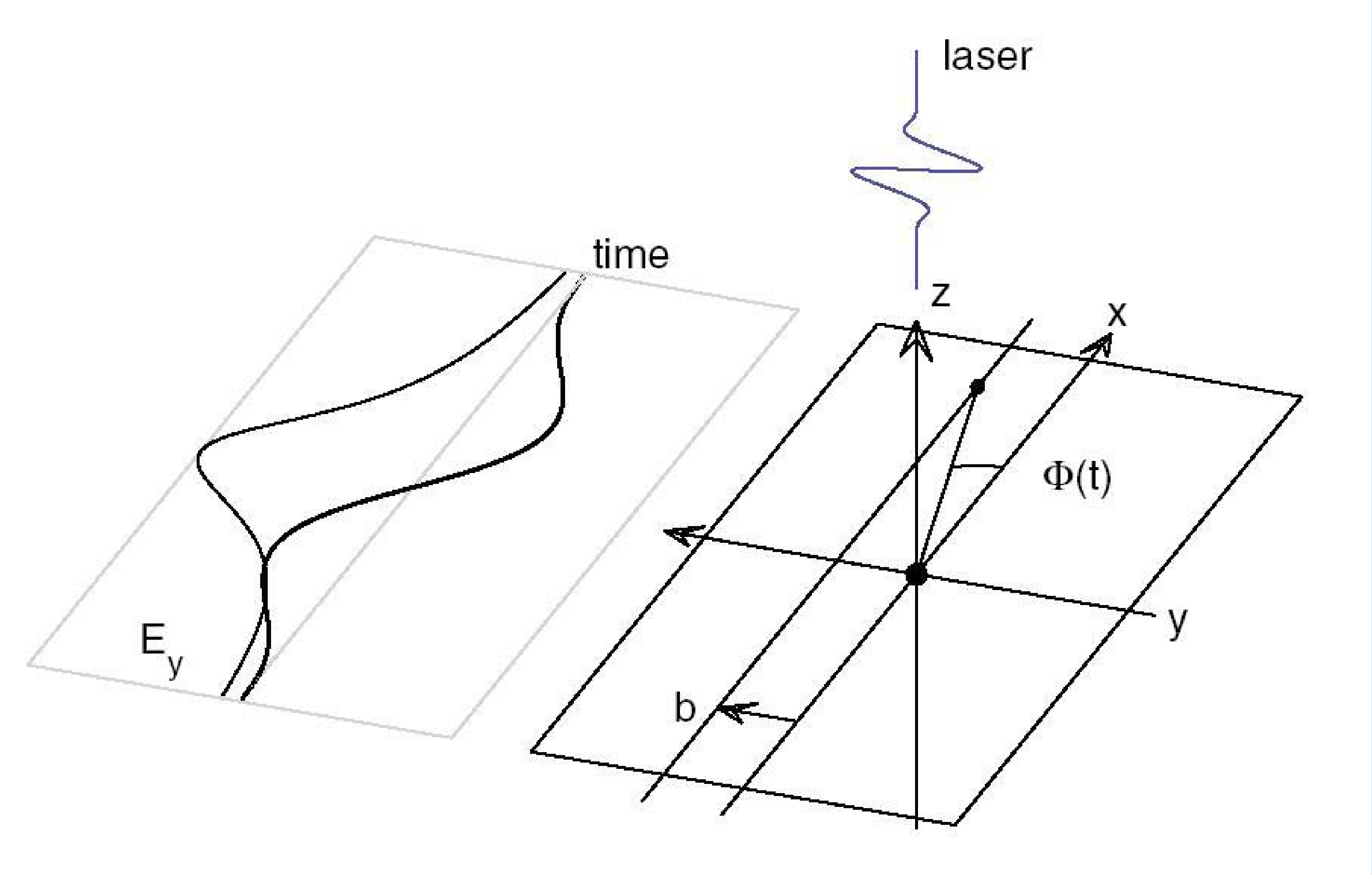

Collision and laser pulse combined

Schrödinger Equation

$$i\partial_t \Psi(\mathbf{r}, t) = H(t)\Psi(\mathbf{r}, t)$$

$$H(t) = h(\mathbf{r}) + V_p(t)$$

Combination of projectile-electron and laser-electron interactions

$$V_p(t) = -\frac{Z_p}{|\mathbf{R}(t) - \mathbf{r}|} - \mathbf{E}(t) \cdot \mathbf{r}$$

Dipole Approximation

$$V_p(t) \approx -\mathbf{r} \cdot [\mathbf{E}(t) + \mathbf{E}_c(t)]$$

$$\begin{pmatrix} i\partial_t c_s \\ i\partial_t c_{p-} \\ i\partial_t c_{p+} \end{pmatrix} = \left[f_{sp}(R) \begin{pmatrix} 0 & \text{c.c.} & \text{c.c.} \\ e^{-i[\Delta E_{sp}(t)-\phi(t)]} & 0 & 0 \\ e^{-i[\Delta E_{sp}(t)+\phi(t)]} & 0 & 0 \end{pmatrix} + \right.$$

$$\left. y_{sp} E_0 f(t) \begin{pmatrix} 0 & \text{c.c.} & \text{c.c.} \\ -e^{i\Delta\varepsilon_{sp}t}\cos(\omega t + \delta) & 0 & 0 \\ e^{i\Delta\varepsilon_{sp}t}\cos(\omega t + \delta) & 0 & 0 \end{pmatrix} \right] \begin{pmatrix} c_s \\ c_{p-} \\ c_{p+} \end{pmatrix}$$

c_s, c_{p-}, c_{p+} are amplitudes for the s, $p_{m=-1}$, and $p_{m=+1}$ states

y_{sp} is the dipole matrix element $\langle s|y|p \rangle$ between s and p states.

Amplitude Equations

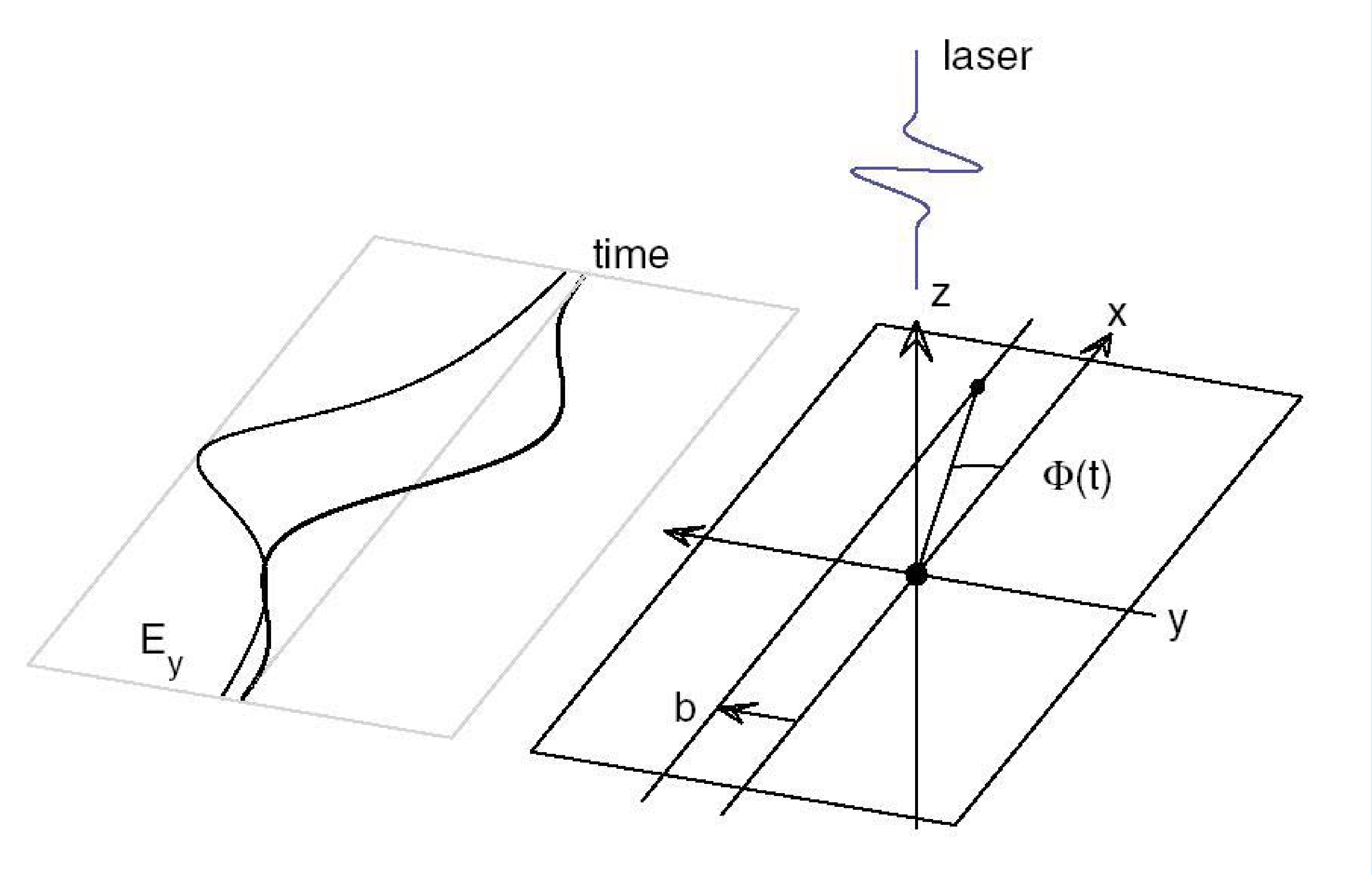

Collision and laser pulse combined

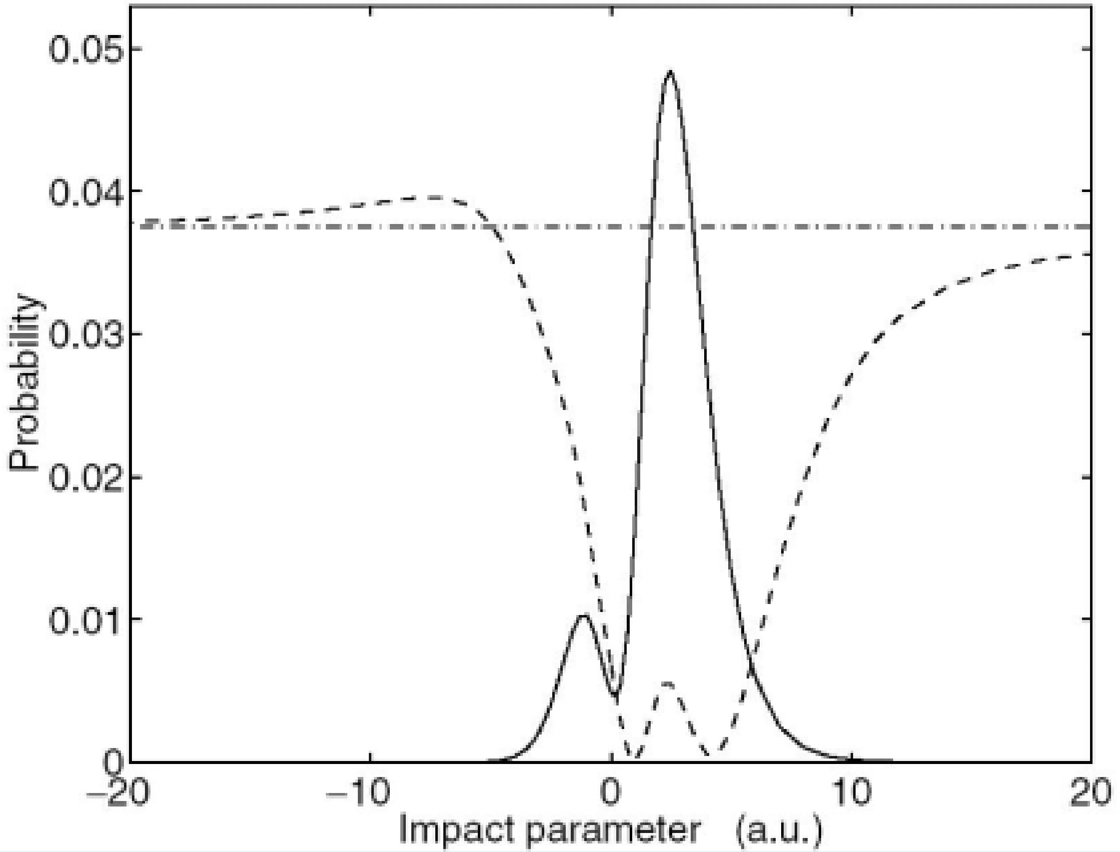

FIG. 2. Excitation probability for H(1s)-H(2p_-) ($Z_p = 1$) in the presence (dashed line) and absence (full line) of a laser pulse. The dot-dashed line is the laser-only contribution. The projectile velocity is $v = 1$ a.u., the duration of the laser pulse is $\tau =$ 0.3 fs, and the peak intensity is set by $y_{sp}E_0 = 0.045$ a.u. (cf. Fig. 4).

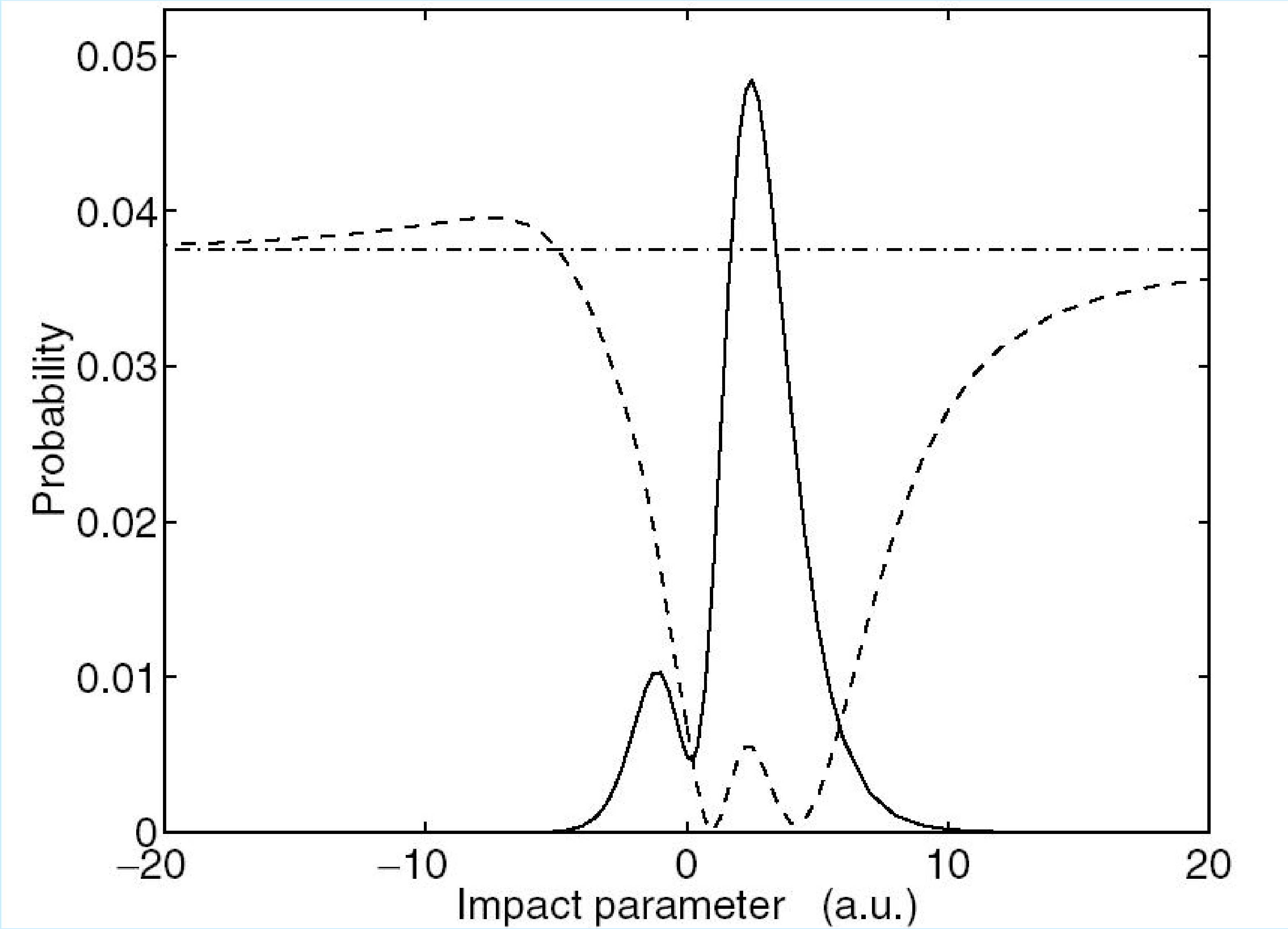

Collisions inside subfemtoseconds laser pulses

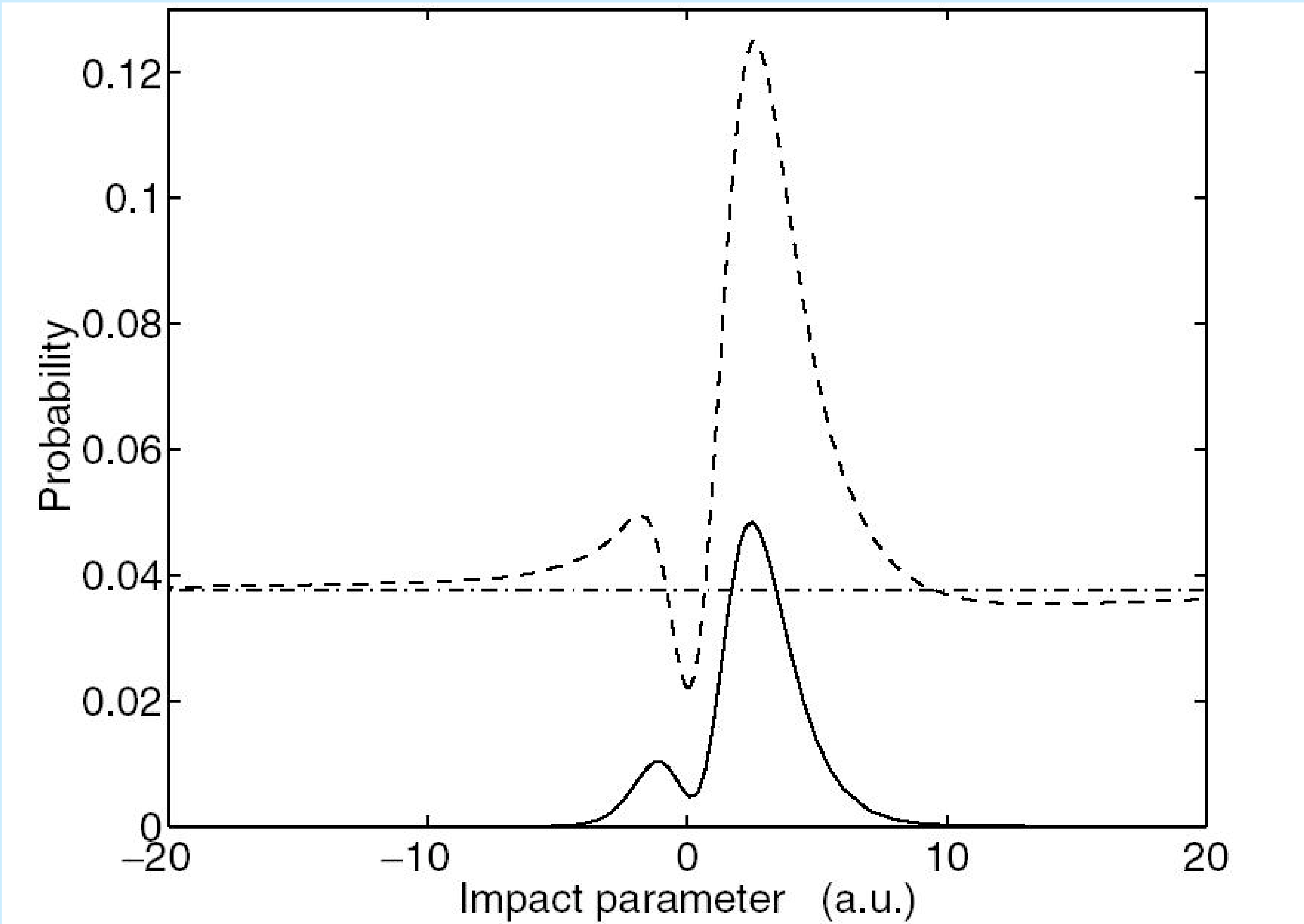

FIG. 3. As Fig. 2, but for constructive interference between the collision and laser interactions (see text).

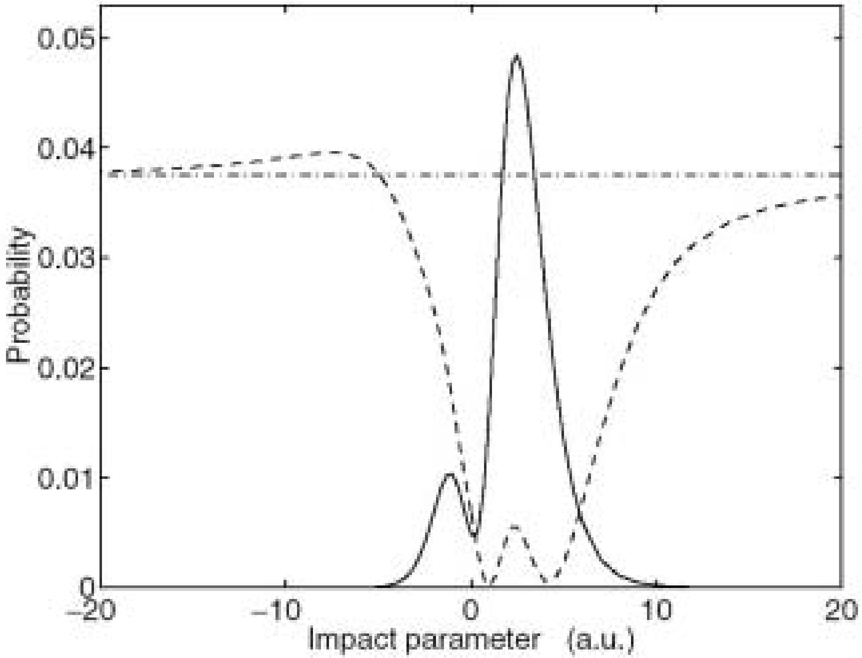

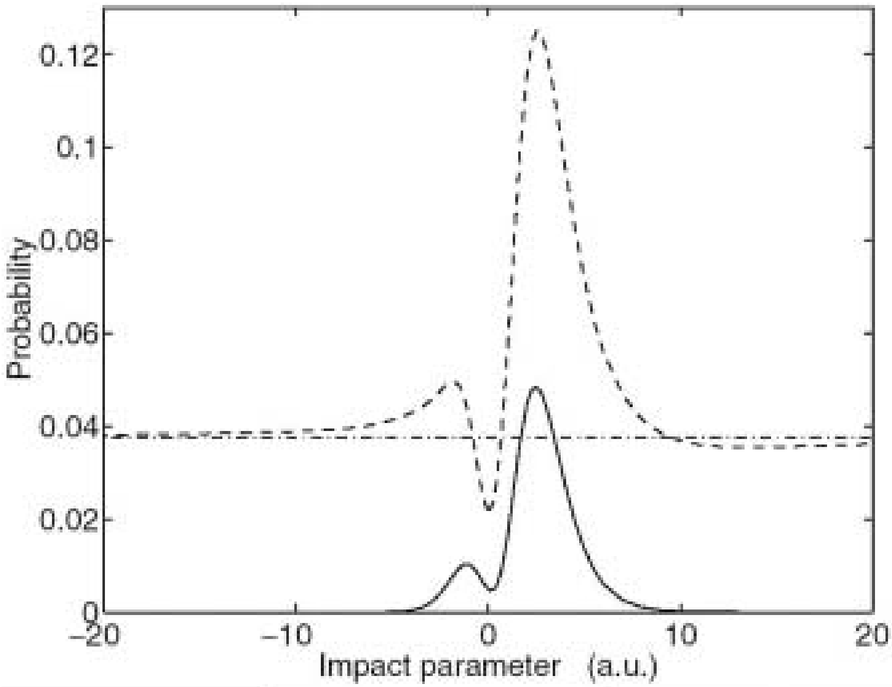

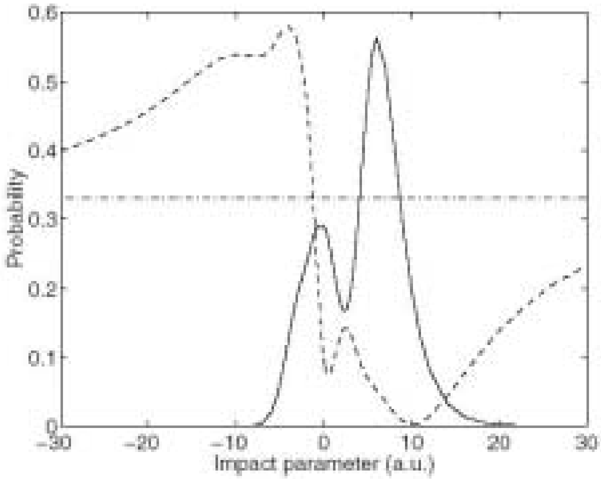

FIG. 4. As Fig. 2, but for Na(3s)-Na(3p_-), $\tau = 1$ fs, and $v = 0.4$ a.u. The peak intensity of the laser is set by $y_{sp}E_0 = 0.1$ a.u., corresponding to the peak value in the collisional strength $f_{sp}(R)$.

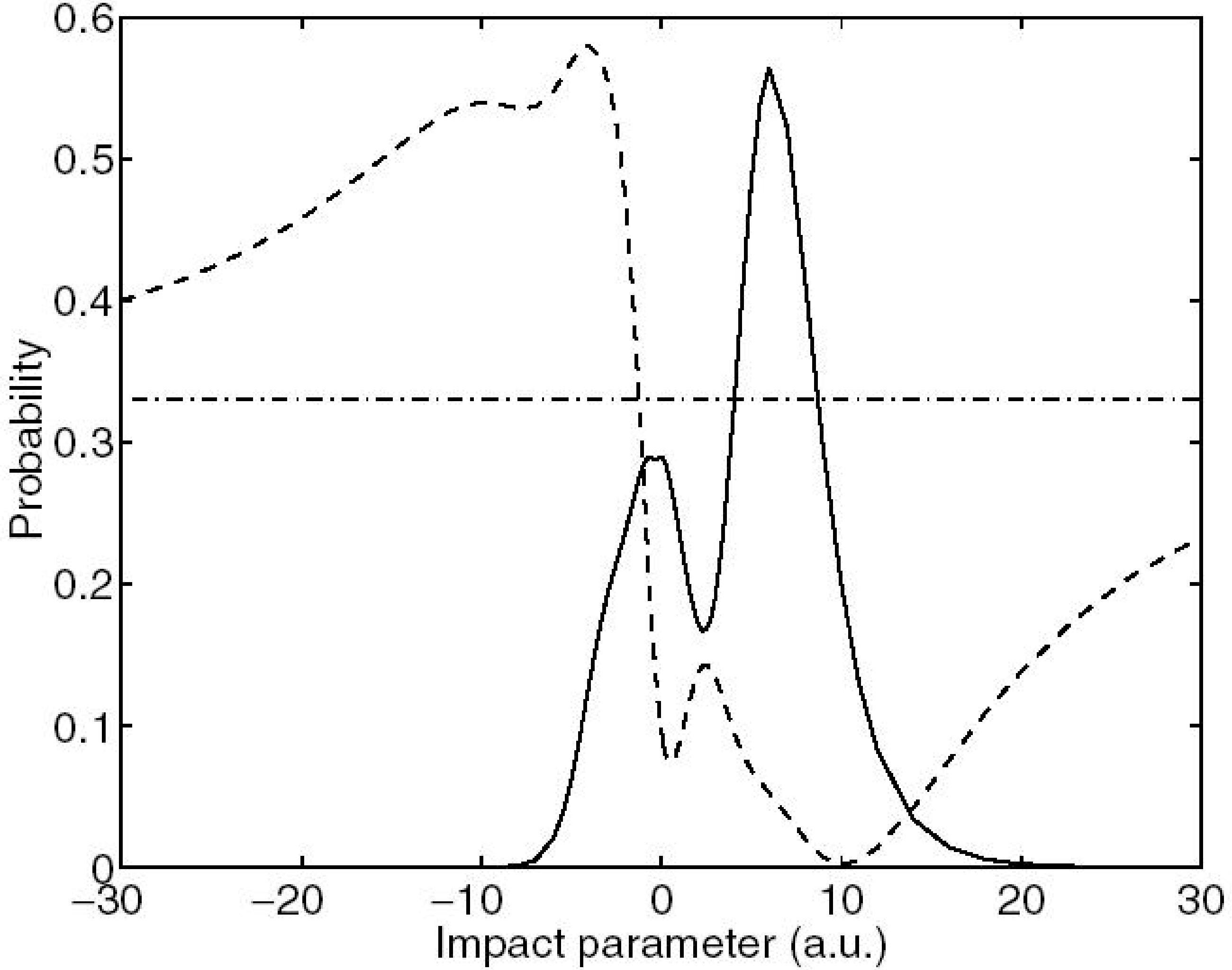

FIG. 4. As Fig. 2, but for Na(3s)-Na(3p_-), $\tau = 1$ fs, and $v = 0.4$ a.u. The peak intensity of the laser is set by $y_{sp}E_0 = 0.1$ a.u., corresponding to the peak value in the collisional strength $f_{sp}(R)$.

Collisions leading to ionization.

One electron is ejected as a result of the collision, the laser pulse, or their combination

Simulated in CTMC

CTMC: Classical Trajectory Monte Carlo model

Newton equations are solved for hundreds of thousands sets of initial conditions

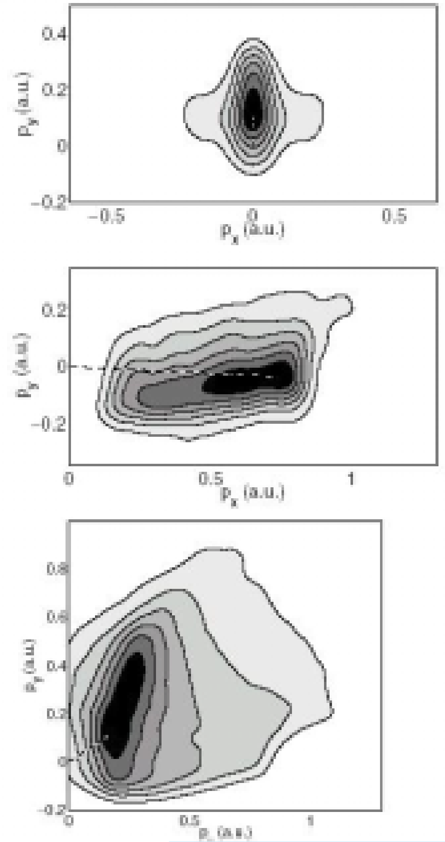

FIG. 5. Distribution of the ejected electron momenta in the collision plane for ionization in p-H(1s). Upper: Laser only. Middle: Collision only. Lower: Collision and laser. The CTMC data have been binned into a 32×32 array and slightly smoothed. Each new shade corresponds to an increase in probability density by 15%. The broken lines indicate the position of the most probable momentum. Parameters as in Fig. 2, except $E_0 = 0.19$ a.u.

Classical (CTMC) simulations of ionization in collisions inside a short laser pulse

Laser only

Collision only

Combination of both

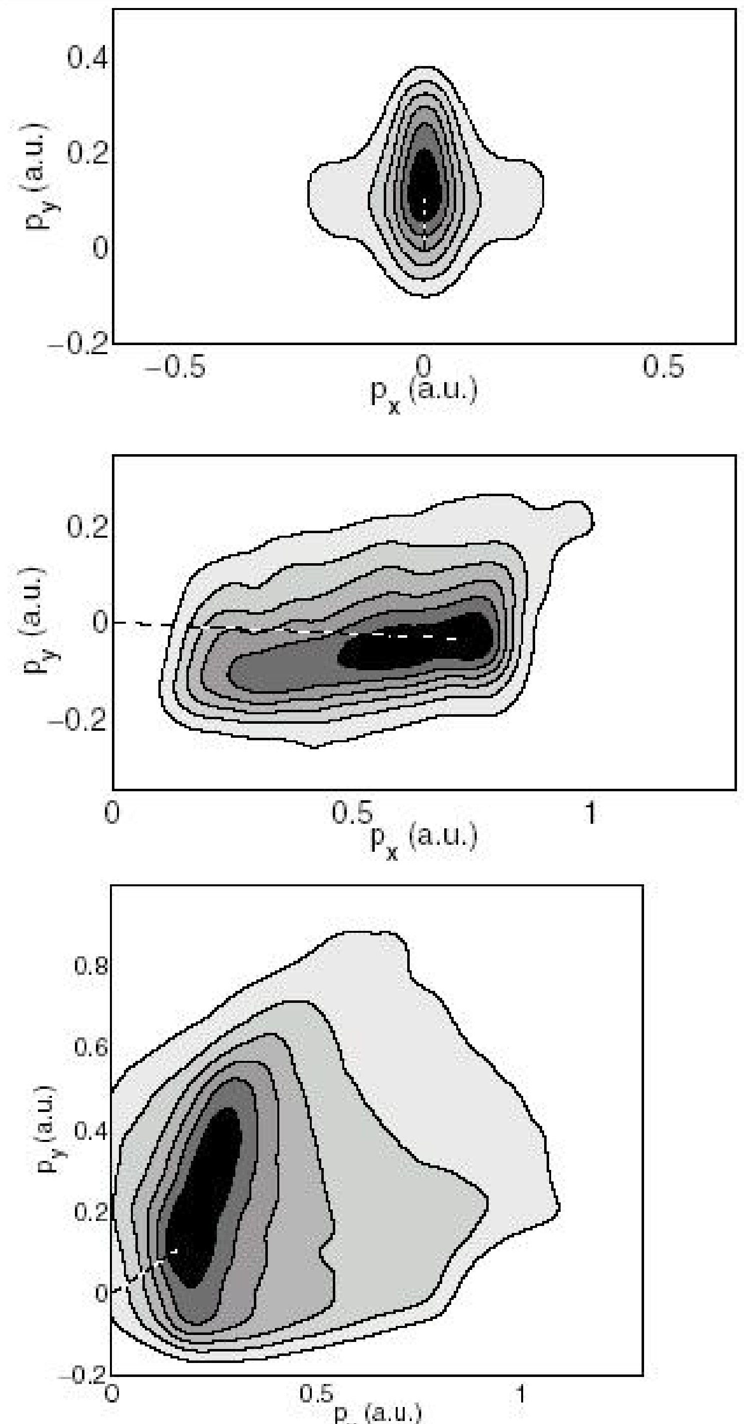

FIG. 5. Distribution of the ejected electron momenta in the collision plane for ionization in p-H(1s). Upper: Laser only. Middle: Collision only. Lower: Collision and laser. The CTMC data have been binned into a 32×32 array and slightly smoothed. Each new shade corresponds to an increase in probability density by 15%. The broken lines indicate the position of the most probable momentum. Parameters as in Fig. 2, except $E_0 = 0.19$ a.u.

Laser pulse only

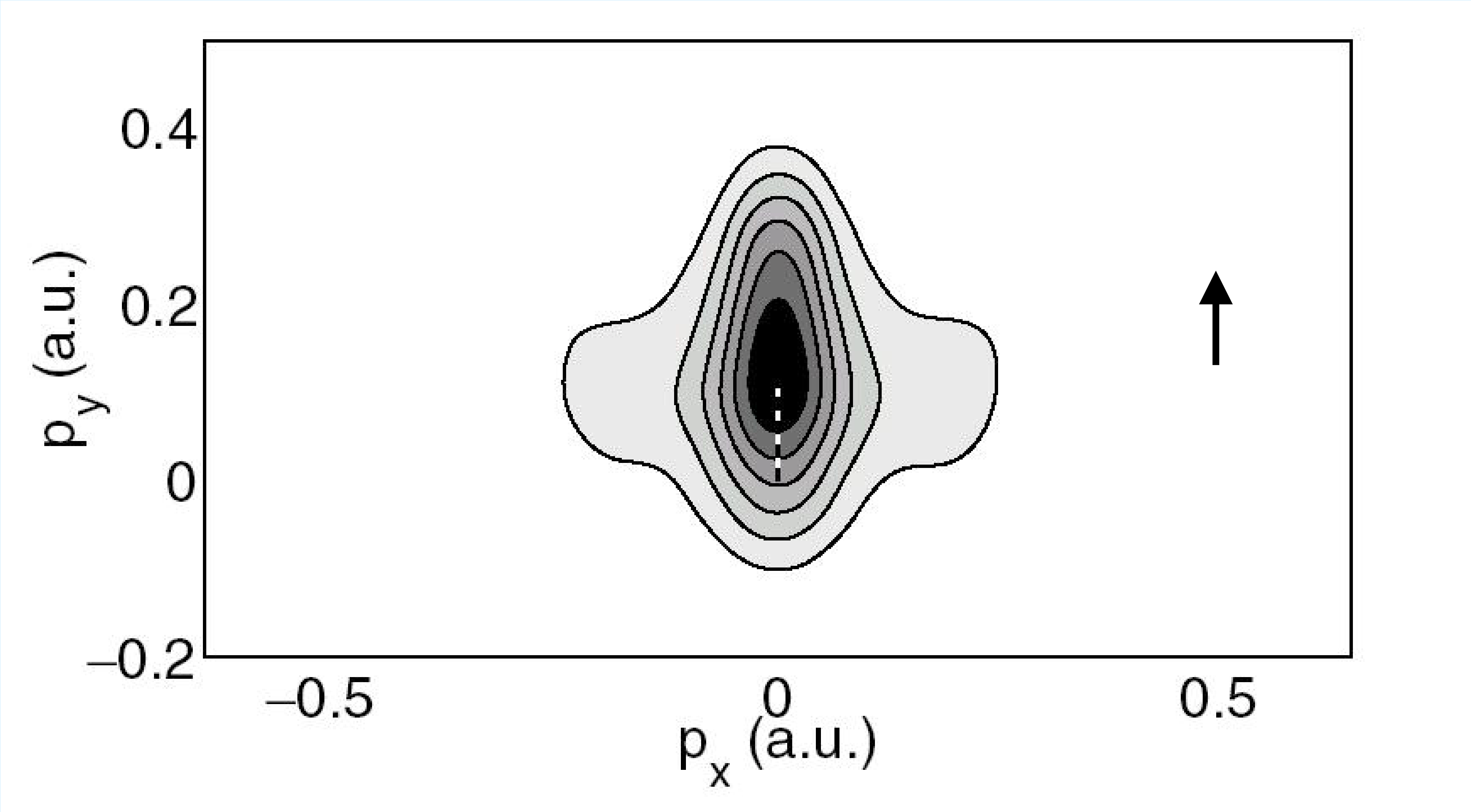

Collision only

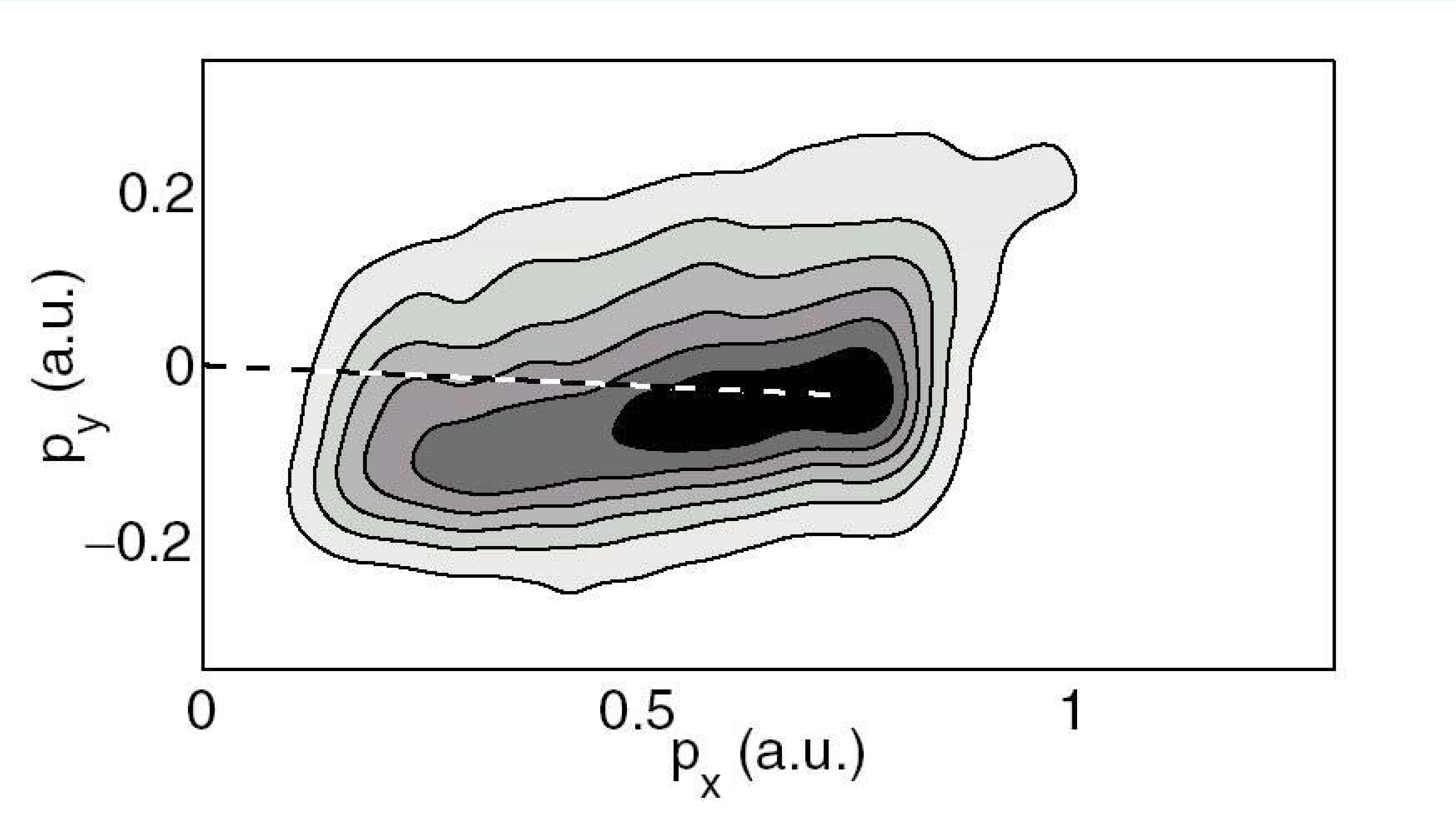

Combination of both laser pulse and collision

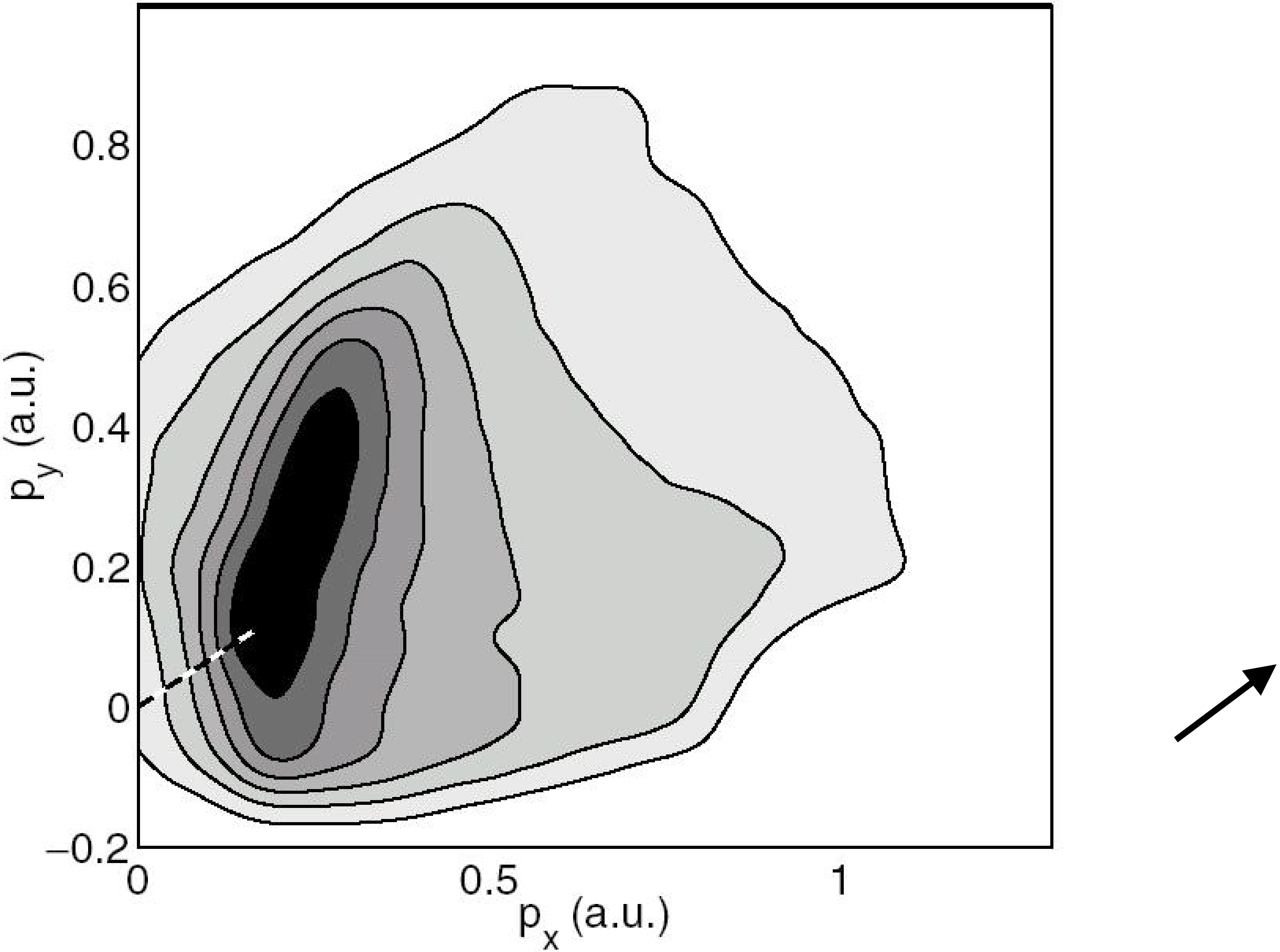

Classical (CTMC) simulations of ionization

Laser only

Collision only

Combination of both

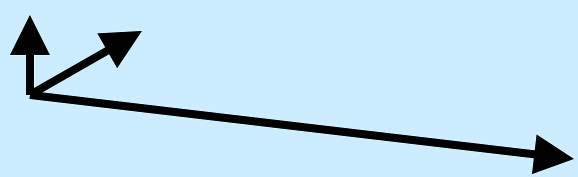

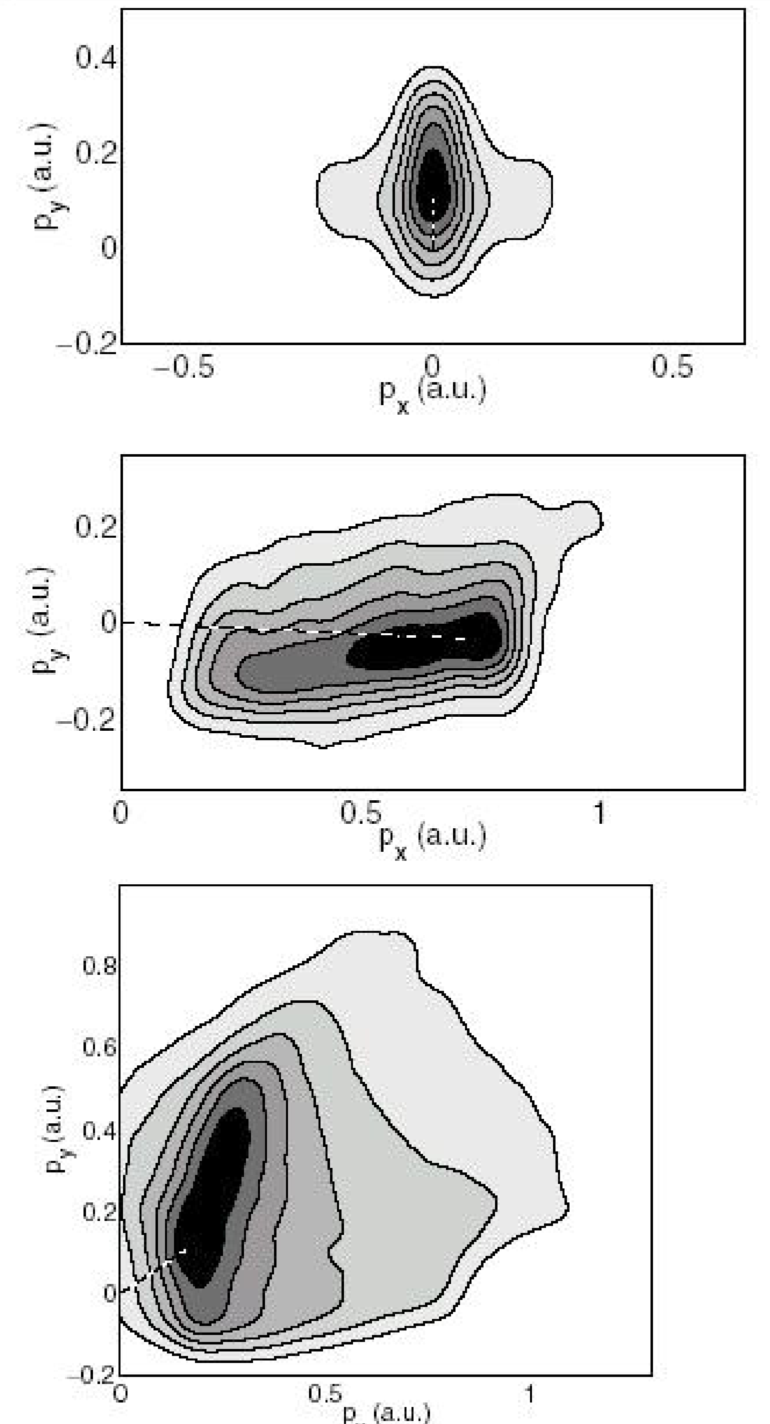

Can this be detected?

COLTRIMS

COLd Target Recoil Ion Momentum Spectroscopy

PES Photon Emission spectroscopy

TES Translational Energy gain Spectroscopy

COLTRIMS

COLd Target Recoil Ion Momentum Spectroscopy

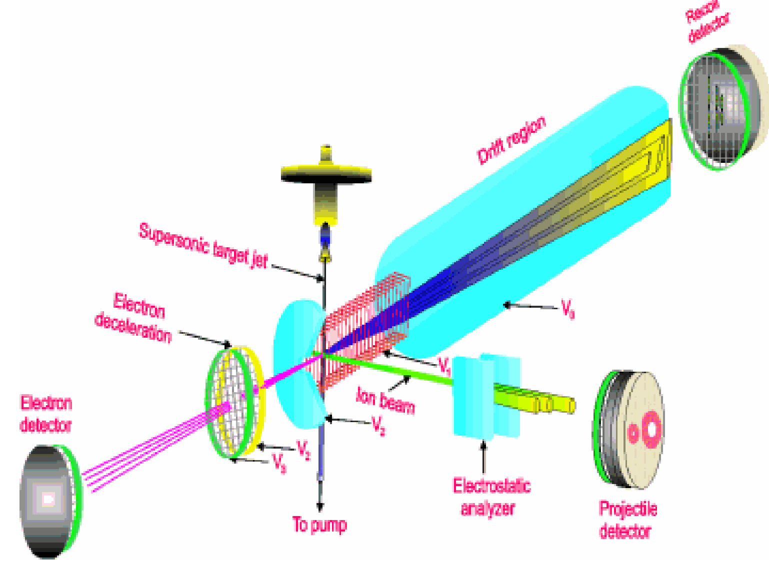

The concept and techniques of COLTRIMS were introduced by the group of Prof. H. Schmidt-Böcking (Frankfurt) just before the 1990's and in particular with the work of J. Ullrich and R. Dörner. By using static 30 K (ΔE =4 meV) gas targets they demonstrated that transverse recoil momenta could be measured corresponding to μRad projectile scattering angles. In the 1990's however, the real breakthrough for COLTRIMS came with the development of the ultra-cold supersonic gas jet (Mergel et al.[41]) and also with sophisticated recoil ion extraction and detection techniques by using electrostatic lenses[42] (Ali et al. , Frohne et al.). These two improvements pushed the resolution of helium recoils to 1.2 μeV (Mergel et al.). Moreover the solid angle for recoil detection increased to 4π.

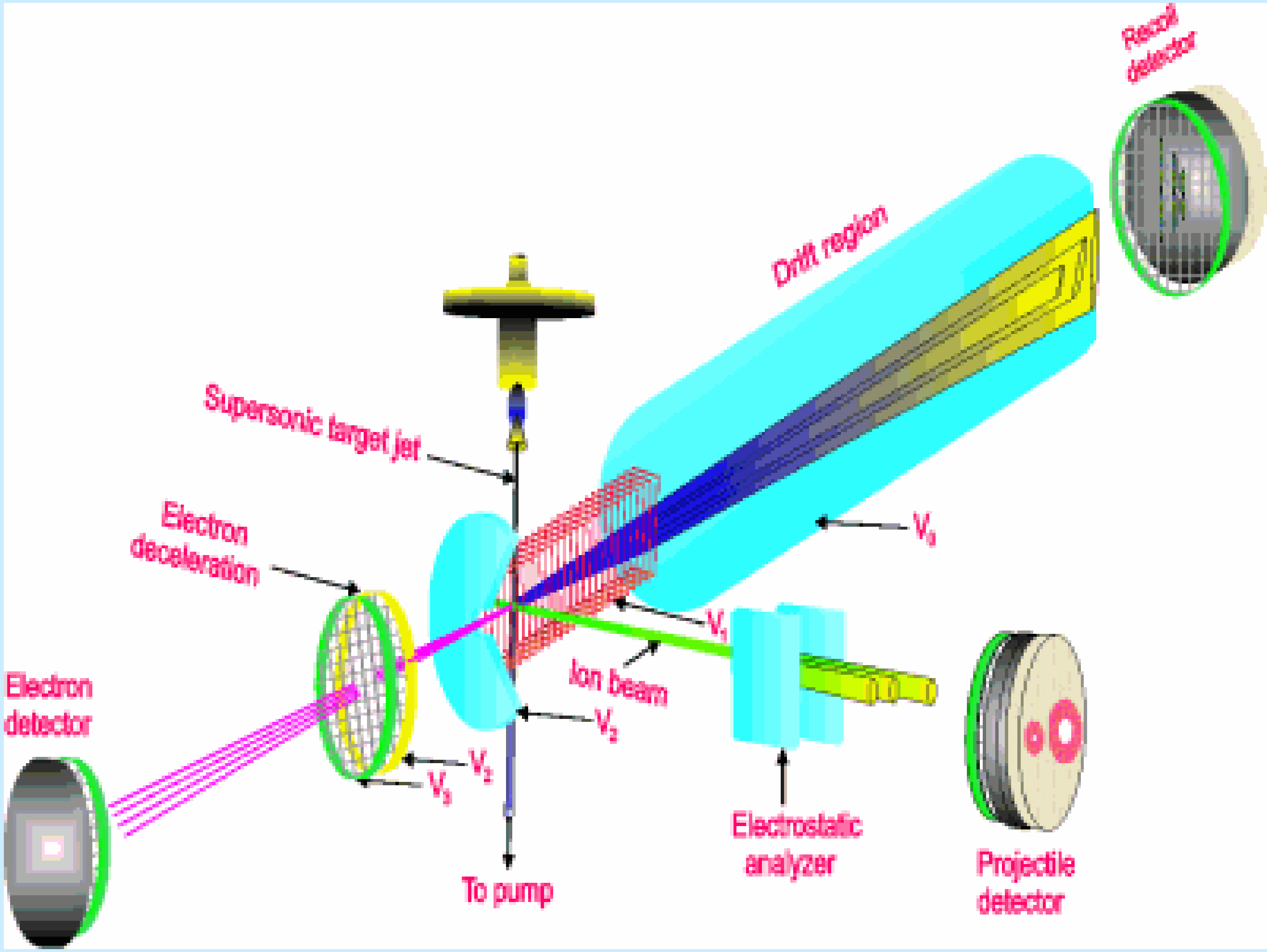
Recoil detector
Drift region
Supersonic target jet
Electron deceleration
Electron detector
V_0
V_1
Ion beam
V_2
V_2
V_3
To pump
Electrostatic analyzer
Projectile detector